

Characterization of converted tin phosphate coating on iron and steel by conversion electron Mössbauer spectrometry (CEMS)

K. NOMURA, Y. UJIHIRA

Faculty of Engineering, The University of Tokyo, Hongo 7-3-1, Bunkyo-ku, Tokyo 113, Japan

R. KOJIMA, M. YOSHIDA

Central Research Laboratories, Nihon Parkerizing Co. Ltd, Ogami 2784, Hiratsuka City, Kanagawa Prefecture 254, Japan

The chemical states of tin in converted tin phosphate coatings on iron and steel and in tin phosphate powders were analysed by conversion electron Mössbauer spectrometry and transmission Mössbauer spectrometry. The tin species in stannous phosphate, stannic oxide and metallic tin were recognized in the converted tin phosphate coatings. Mössbauer parameters of Sn(II) included in the phosphate coatings were slightly different from those of Sn(II) incorporated in powders of zinc and manganese phosphate compounds. The tin atoms mainly occupied two different sites in three sites of stannous phosphate structure, depending on the preparations.

1. Introduction

Zinc or manganese phosphating has widely been used as a surface treatment of iron and steel [1]. Crystalline fitting of phosphate compounds on iron was studied by Gebhardt [2]. The chemical states of iron included in phosphate coatings [3] and in the thermal decomposition products of phosphate coatings [4] have been analysed and characterized by conversion electron Mössbauer spectrometry (CEMS) and conventional transmission Mössbauer spectrometry (TMS). The growth of phosphophyllite, $Zn_2Fe(PO_4)_2 \cdot 4H_2O$ [5], and hureaulite, $(Mn, Fe)_5H_2(PO_4)_4 \cdot 4H_2O$ [6, 7], has been studied in zinc phosphate and manganese phosphate coatings, respectively. The site distributions of iron in the other iron phosphate compounds were analysed by Mattievich and Danon [8]. Improvement of zinc phosphate coatings was first carried out by Tuttle and Navoy [9], by dipping in stannous chloride solution.

Zinc phosphate coatings are formed on iron and steel, and then part of the coatings is converted into tin phosphate, because tin phosphate cannot be deposited on iron and steel directly by an immersion process. The converted tin phosphate coatings produced by this process are pale grey and are useful for dyeing and lubricant purposes. A salt spray test of manganese phosphate coatings and its converted tin phosphate coatings with paints verified that the durable time of the lubricant was about three times longer for the latter converted tin phosphate coatings than for the former [10].

Stannous phosphates are considered to have far more corrosion resistance than zinc and manganese phosphates because the conversion of zinc or mangan-

ese phosphate coatings to tin phosphate coatings can be carried out in an acid solution of pH 1–3. However, the structure and chemical state of tin in converted tin phosphate coatings have not yet been sufficiently clarified. In the present work, the converted tin phosphate coatings obtained by the treatment of zinc and manganese phosphate coatings in stannous chloride solution were characterized mainly by CEMS, and some stannous phosphate compounds were also analysed using TMS in order to compare them with tin compounds produced in the converted tin phosphate coatings.

2. Experimental procedure

Zinc phosphate coatings and manganese phosphate coatings were prepared by the procedure reported previously [3]. The thickness of the zinc and manganese phosphate coatings was about 3.4 and 9.8 $g\ m^{-2}$, respectively. These samples were immersed in a hot solution ($> 90^\circ C$) of 2.5% stannous chloride, containing tartaric acid and hydrochloric acid for 2 min. Powders of hopeite, $Zn_3(PO_4)_2 \cdot 4H_2O$, phosphophyllite and hureaulite were prepared by a precipitation method [6]. Hot drops of stannous chloride solution were added to the phosphate powders thus prepared, and the powders were washed with water to remove soluble products. Tin phosphate was prepared by adding stannous chloride in a hot phosphate solution, and anhydrous tin phosphate was prepared by heating the precipitated tin phosphate in an atmosphere of 5% $H_2 + 95\% N_2$ gas at 810 K for 100 min. These samples were used to compare the Mössbauer parameters of tin compounds produced in the phosphate coatings.

CEM spectra were observed by a back-scatter type electron detector made by the authors [11], with a flowing mixture of 95% He and 5% CH₄, coupled to a Mössbauer spectrometer. About 10 MBq of ^{119m}Sn (BaSnO₃) source and 1 GBq of ⁵⁷Co(Rh) were used. The Doppler velocity was calibrated using BaSnO₃ and α-Fe.

3. Results and discussion

3.1. Chemical states of tin in converted tin phosphate coatings

The scanning electron micrographs of zinc and manganese phosphate coatings modified by stannous

chloride solution and further treated in a chromate solution of 5% CrO₃ are shown in Figs 1 and 2, together with micrographs of zinc and manganese phosphate coatings as-prepared, respectively. The crystalline shapes of these phosphate coatings changed after treatment of stannous chloride solution, but the new crystalline shapes of the converted tin phosphate coatings remained stable after treatment in the chromate solution, while zinc and manganese phosphate coatings without treatment in stannous chloride could be removed in the chromate solution at 70 °C. This shows that the converted tin phosphate coatings could have a strong resistance to corrosion in

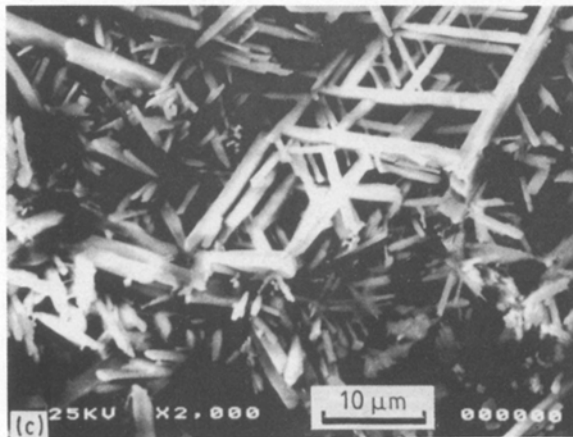
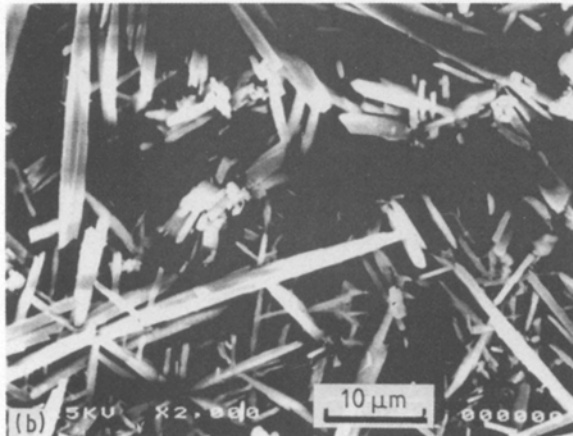
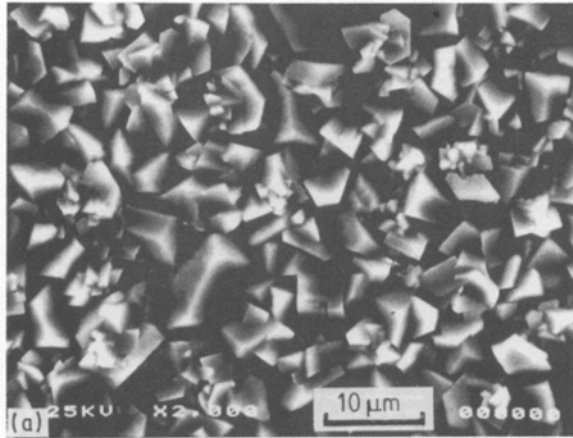


Figure 1 Scanning electron micrographs of manganese phosphate coatings (a) before and (b) after the treatment in stannous chloride solution, and (c) the converted tin phosphate coating treated further in chromate solution.

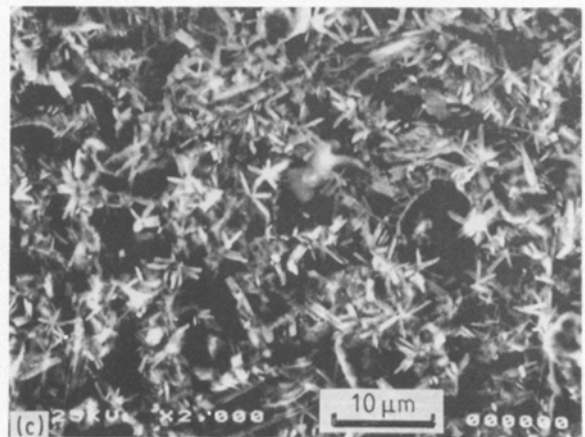
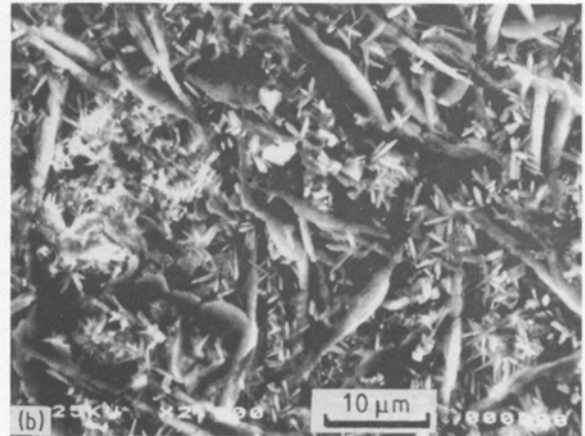
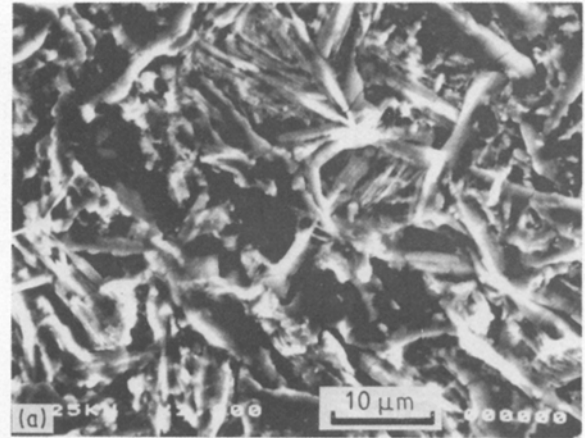


Figure 2 SEM images of zinc phosphate coatings (a) before and (b) after the treatment in stannous chloride solution, and (c) the converted tin phosphate coating treated further in chromate solution.

an acid medium. The CEM spectra of manganese phosphate and zinc phosphate coatings, treated with stannous chloride solution, are shown in Fig. 3. Sn(II) and Sn(IV) species were observed in the CEM spectra of both samples. Sn(II) atoms in stannous phosphate occupy three sites, of which two are similar. The average distances between tin atoms and oxygen atoms are 0.21 and 0.223 nm. Peaks of Sn(II) species in the CEM spectrum observed were also deconvoluted into two doublets. In all, two doublets of Sn(II), a doublet of Sn(IV) and a singlet of tin atoms with $5s5p^3$ mixed orbitals were observed in the CEM spectrum of the converted tin phosphate coating of manganese phosphate. The isomer shift, IS, of the singlet was close to α -Sn rather than β -Sn. The Mössbauer parameters (IS, quadrupole splitting, QS, and the intensity ratios) were slightly different from those of the converted tin phosphate coating of zinc phosphate, as shown in Table I. X-ray diffraction analysis of the converted tin phosphate coating of manganese phosphate con-

firmed the presence of species similar to $\text{Sn}_3(\text{PO}_4)_2$, and trace amounts of SnHPO_4 and $\text{Sn}_2\text{Cl}(\text{PO}_4)$. Tin phosphate compounds were found to be produced by substitution in part of the manganese and zinc phosphate coatings. Although SnO_2 could not be clearly detected in X-ray diffraction patterns, peaks of Sn(IV) species were clearly observed in the CEM spectra of converted tin phosphate coatings of manganese and zinc phosphates. It was considered that Sn(IV) species produced by hydrolysis of stannous chloride was weakly adhesive on the top layers of zinc and manganese phosphate coatings.

CEM spectra of converted tin phosphate coatings, produced by dipping zinc phosphate coatings in stannous chloride solutions of pH2 at 95 °C for 1 min, or 87 °C for 2 min, and pH = 3.2 at 40 °C for 10 min, are shown as Fig. 4. Although peaks of Sn(II) species were not divided especially into two doublets, the intensity ratio of Sn(IV) and Sn(II) species produced in the converted tin phosphate coatings depended on the

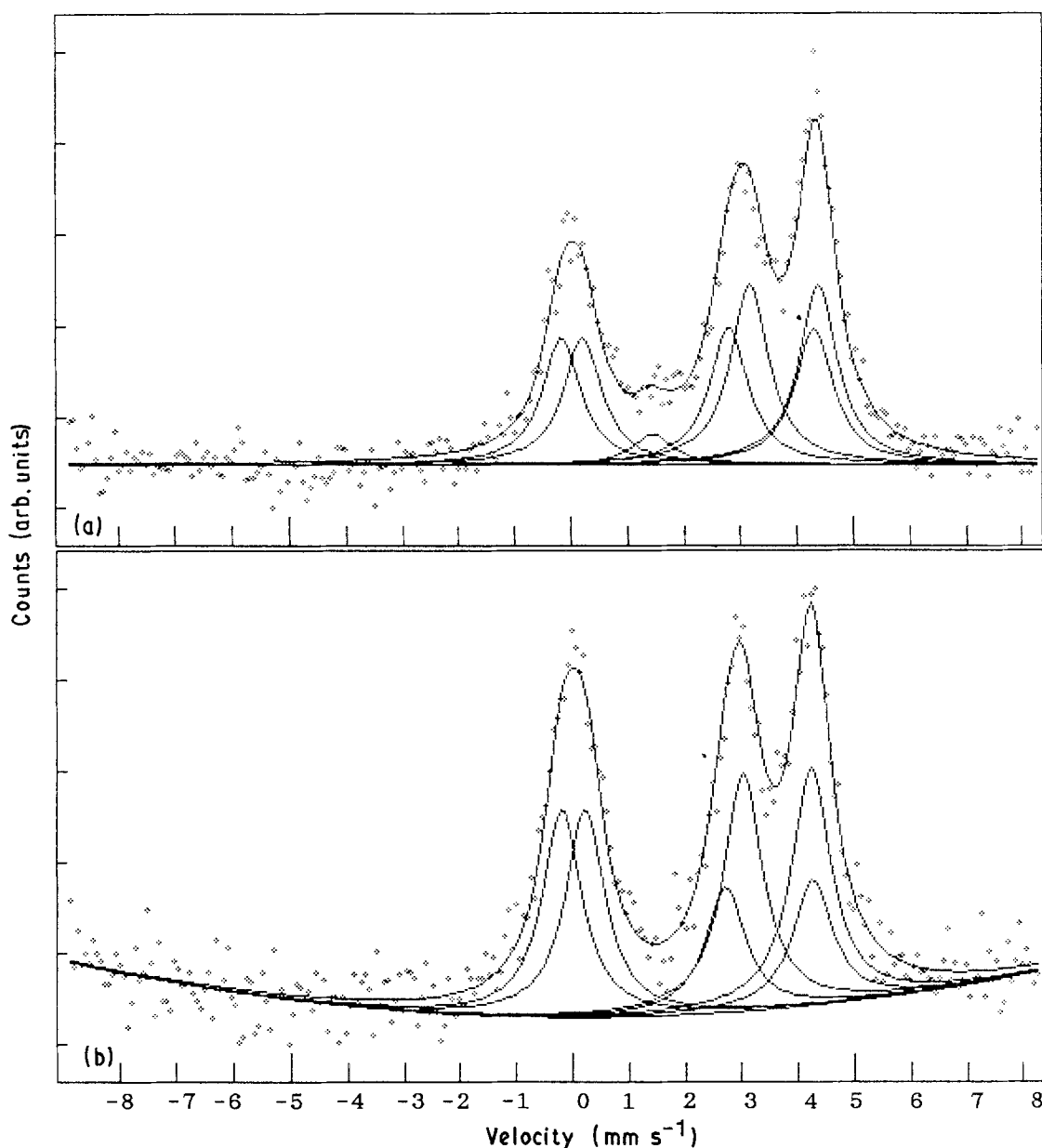


Figure 3 ^{119}Sn conversion electron Mössbauer spectra of (a) manganese phosphate coating, and (b) zinc phosphate coating, treated in stannous chloride solution.

TABLE I ^{119}Sn Mössbauer parameters of converted tin phosphate coatings and powders

Sample matrix	CEMS/TMS	IS (mm s^{-1})	QS (mm s^{-1})	Ratio (%)
Mn phosphate	CEMS	3.54	1.51	29.8
		3.76	1.21	39.2
		1.45	–	6.8
		0.01	0.37	27.6
Zn phosphate	CEMS	3.48	1.55	22.0
		3.61	1.20	41.5
		0.02	0.44	24.8
Metallic Sn phosphate	CEMS	3.01	1.69	42.9
		3.15	1.43	23.4
		2.55	–	20.1
		0.01	0.27	13.6
Hureaulite	TMS	3.38	1.39	53.6
		3.51	1.13	46.4
Phosphophyllite	TMS	3.21	2.27	18.2
		3.70	1.31	81.7
Sn, Zn (1:4) phosphate	TMS	3.51	1.57	30.5
		3.68	1.25	53.4
		– 0.01	0.42	16.0
Sn, phosphate + tartaric acid	TMS	3.12	1.93	79.4
		3.54	0.90	20.6
Sn phosphate	TMS	3.46	1.73	18.5
		3.72	1.37	62.0
		– 0.01	0.48	19.5
Sn phosphate 810 K H_2 ann.	TMS	3.14	2.06	86.0
		3.80	1.56	14.0

immersion conditions. In the films produced by the latter conditions, large amounts of Sn(IV) species and small amounts of stannous phosphate were recognized. These converted tin phosphate coatings were not good enough to be easily stripped off. The peak ratio of Sn(IV) to Sn(II) may be practically useful in the estimation of converted tin phosphate coatings produced by immersion in stannous solution.

3.2. Phosphating of metallic tin

Tin foil (0.1 mm thick) was dipped in 0.1 M H_3PO_4 at 70 °C, dried at room temperature, and CEM and TM spectra of the treated tin foil were measured as shown in Fig. 5. Peaks of tin compounds produced by treatment in phosphoric acid solution did not appear in the TM spectrum. The layers of the products were estimated to be less than 2 μm thick. The doublets of Sn(II) were attributed to $\text{Sn}_3(\text{PO}_4)_2 \cdot x\text{H}_2\text{O}$ and the doublet of Sn(IV) to SnO_2 . These showed almost the same results as did the converted tin phosphate coatings, although Mössbauer parameters of tin phosphate compounds were slightly different from those of converted tin phosphate coatings. It is considered that, while part of stannous ions dissolved by phosphoric acid react with phosphate ions, the other stannous ions are oxidized to form stannic oxide while drying. Mixed compounds of insoluble stannous phosphate and stannic oxide are also deposited on the substrate of metallic tin.

3.3. Depth profiles of converted tin phosphate coatings

^{57}Fe CEM spectra of iron in zinc phosphate coatings before and after treatment in stannous chloride solu-

tion are shown in Fig. 6. A large doublet, due to Fe(II) species of phosphophyllite [4], and a sextet of the iron substrate were observed. After treatment, the intensity of the Fe(II) peaks of phosphophyllite decreased, but no peaks of iron products other than phosphophyllite were clearly observed.

The depth profiles of modified manganese phosphate and zinc phosphate coatings with stannous chloride were carried out by glow discharge emission spectrometry (GDS) and the results are shown in Figs 7 and 8, respectively. Manganese and zinc atoms were substituted for tin atoms in about one-third of the top surface layers, respectively, because the intensity of the phosphorus atoms did not change very much before and after treatment in stannous chloride solution. The GDS results showed that the concentration of tin atoms increased on the top surface layers of these phosphate coatings. X-ray photoelectron spectra of these samples are shown in Fig. 9. Peaks of stannous phosphate appeared at 487 eV (binding energy of Sn 3d electrons), and peaks of tin(IV) shifted to 491 eV due to charging. It was reconfirmed that SnO_2 was only adhesive on the top layers. The right shoulder of the stannous phosphate peak was observed at 485 eV in deeper layers, which might correspond to the metallic state of the tin observed in CEM spectra as small peaks. The metallic state of tin was considered to be produced by reducing part of the stannous ions reaching the iron substrate.

3.4. Site distribution of tin in converted phosphate powders

Fig. 10 shows ^{119}Sn Mössbauer spectra of powders obtained by dropping a hot stannous chloride solution into manganese hureaulite and phosphophyllite,

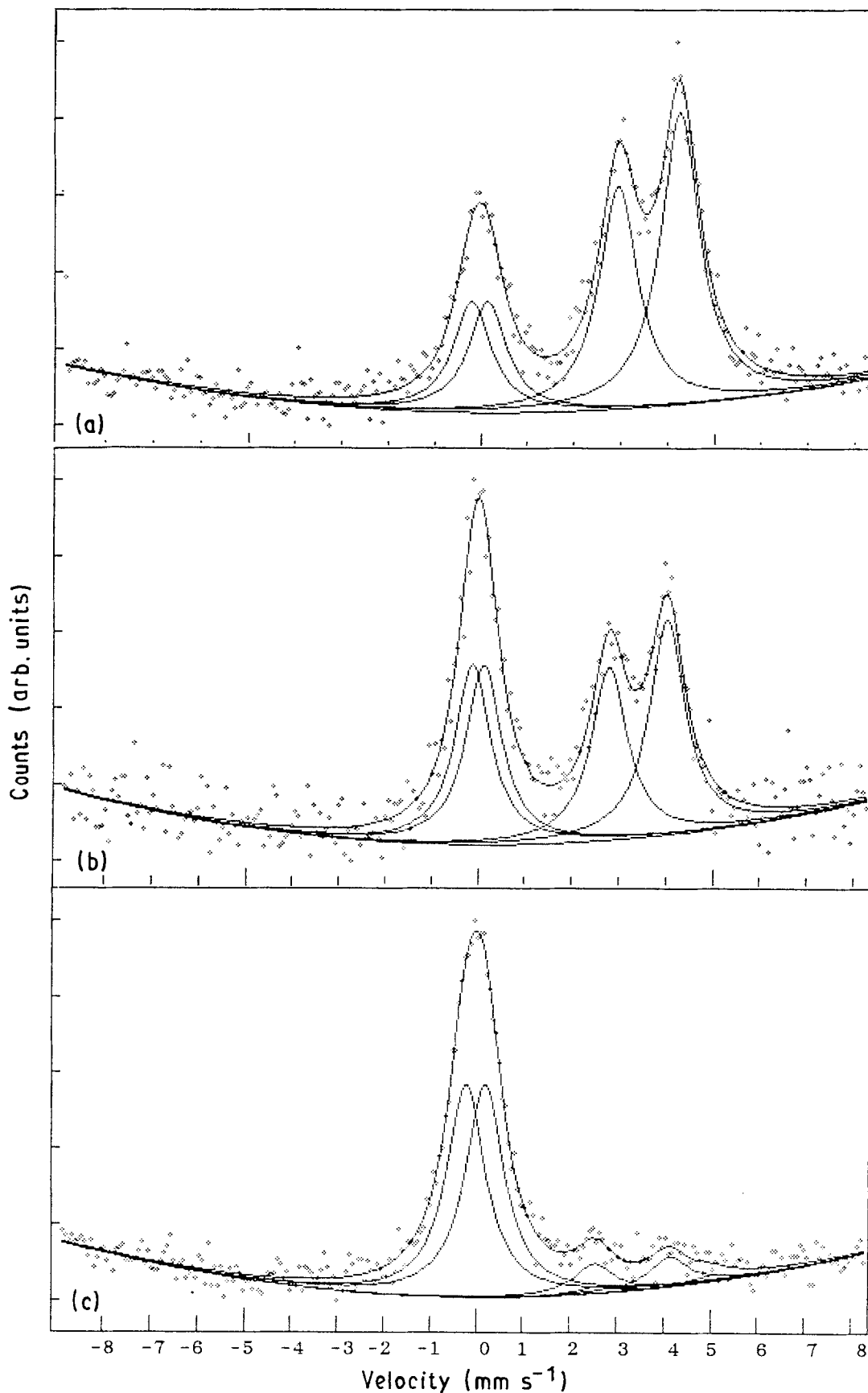


Figure 4 ^{119}Sn CEM spectra of zinc phosphate coating, treated in stannous chloride solution of (a) pH = 1.8 at 95°C for 1 min, (b) pH = 2 at 87°C for 2 min, and (c) pH = 3.2 at 40°C for 10 min.

and of tin phosphate powder precipitated by adding stannous chloride solution containing tartaric acid to a phosphate solution; Fig. 11 shows tin phosphate prepared by precipitation and the annealed sample at 810 K. Mössbauer parameters differed slightly among

these samples. The tin atoms in stannous phosphate produced in precursor phosphate compounds are considered to occupy two different sites of the three stannous phosphate sites, depending on the kind of precursor phosphate compounds and the preparation

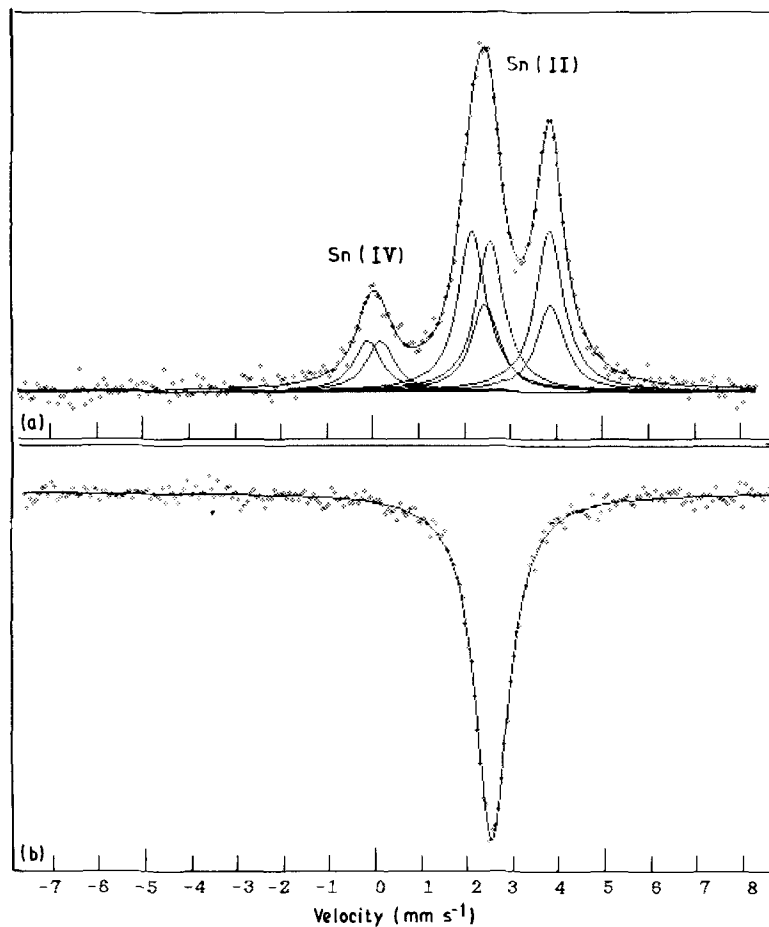


Figure 5 ¹¹⁹Sn CEM and TM spectra of tin foil treated in phosphate solution.

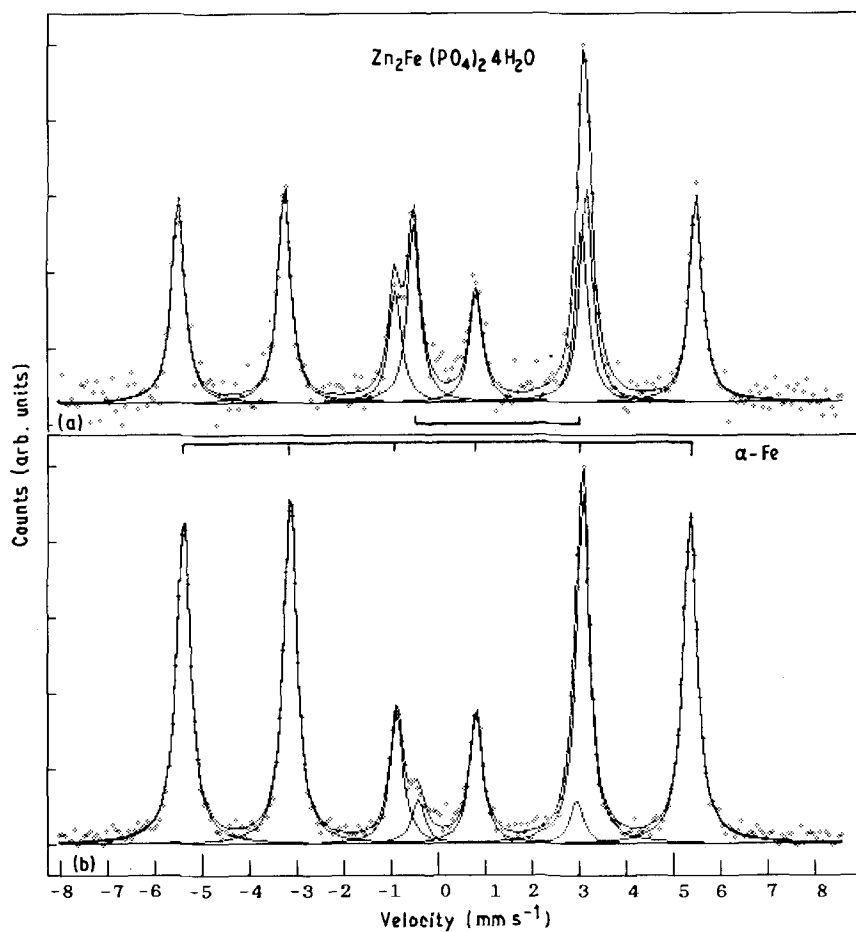


Figure 6 ⁵⁷Fe CEM spectra of zinc phosphate coating (a) before and (b) after treatment with stannous chloride solution.

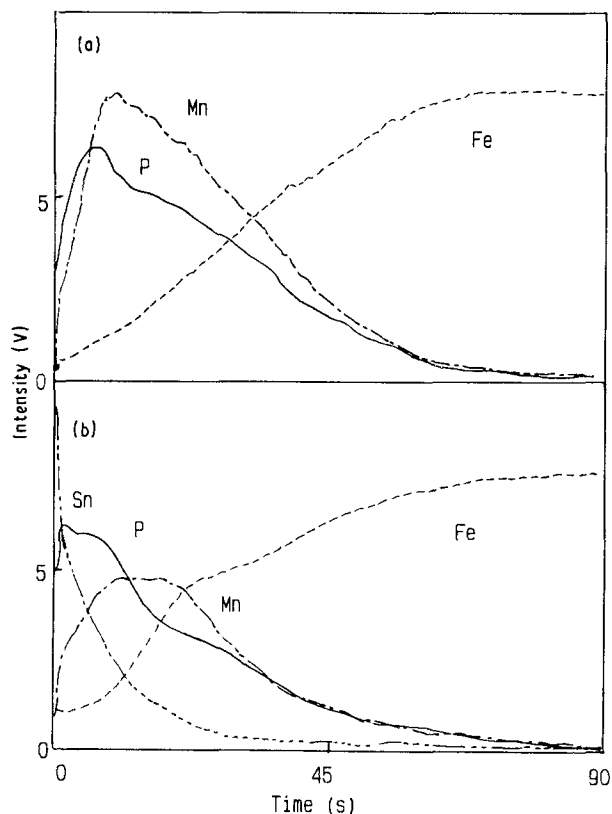


Figure 7 Depth profiles of manganese, tin, iron and phosphorus in manganese phosphate coating (a) before and (b) after treatment in stannous chloride solution by glow discharge emission spectrometer (GDS).

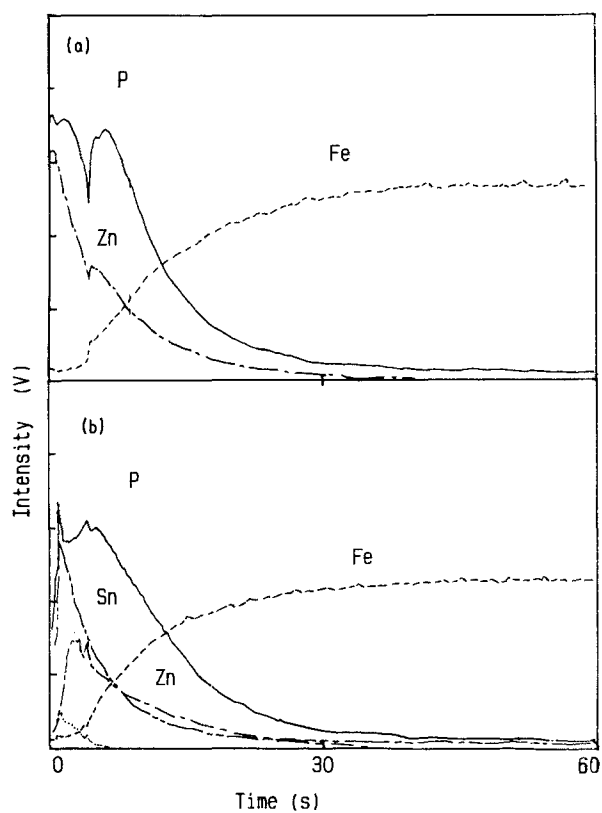


Figure 8 Depth profiles of zinc, tin, iron and phosphorus in zinc phosphate coating (a) before and (b) after treatment in stannous chloride solution by glow discharge emission spectrometry.

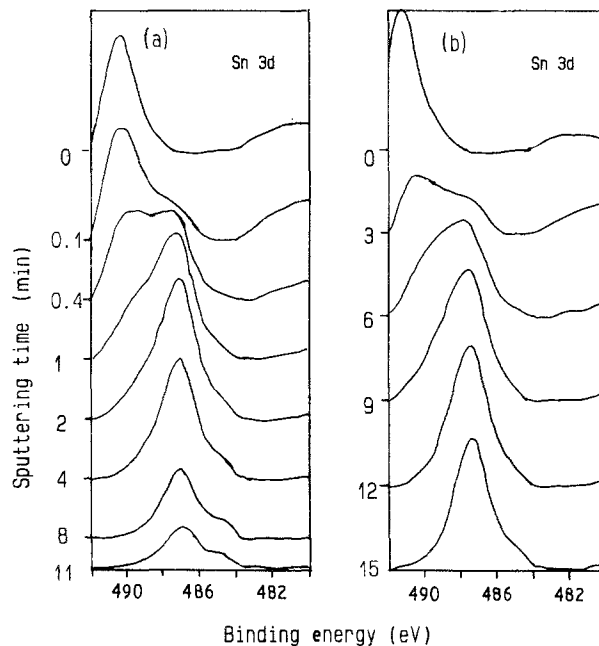


Figure 9 XPS spectra of tin (3d electrons) in (a) manganese phosphate coating and (b) zinc phosphate coating, treated in stannous chloride solution.

conditions used. It is known that the IS value of stannous compounds increases with decreasing QS value and the 5p electron density for $5s5p^3$ configurations of tin [12]. The 5p electron density of tin atoms in zinc and manganese phosphate matrices decreased compared with that of anhydrous stannous phosphate, which crystallizes in monoclinic structure. The Mössbauer parameters of anhydrous $\text{Sn}_3(\text{PO}_4)_2$ obtained differed from those reported previously by Mercader *et al.* [12] ($\text{IS}_1 = 2.92 \text{ mm s}^{-1}$, $\text{QS}_1 = 1.85 \text{ mm s}^{-1}$ and $\text{IS}_2 = 3.53 \text{ mm s}^{-1}$, $\text{QS}_2 = 1.49 \text{ mm s}^{-1}$). The average values of two doublets of anhydrous stannous phosphate obtained in our experiments were similar to the published data ($\text{IS} = 3.06 \text{ mm s}^{-1}$, $\text{QS} = 1.93 \text{ mm s}^{-1}$ [13] and $\text{IS} = 3.05 \text{ mm s}^{-1}$, $\text{QS} = 1.90 \text{ mm s}^{-1}$ [14]), which has been analysed previously by the same authors as a single doublet. In many stannous phosphates prepared, an Sn(II) species with $\text{IS} \approx 3.6 \text{ mm s}^{-1}$ and $\text{QS} \approx 1.4 \text{ mm s}^{-1}$ was often observed as a main constituent and Sn(II) species with $\text{IS} \approx 3.1 \text{ mm s}^{-1}$ and $\text{QS} \approx 1.9 \text{ mm s}^{-1}$ was sometimes observed. Two doublets with a large QS ($\sim 1.9 \text{ mm s}^{-1}$) and with a small QS ($\sim 1.5 \text{ mm s}^{-1}$) could not always be contained with a constant ratio. The published data for stannous phosphate are considered to have been inconsistent because tin atoms occupy preferentially two out of the three sites of tin atoms in stannous phosphate structure, depending on the preparation methods.

4. Conclusions

It was found that converted stannous phosphate and adsorbed SnO_2 species were mainly produced in about the top one-third of the layers of manganese and zinc phosphate coatings, and that of metallic tin was sometimes detected in deeper layers. The

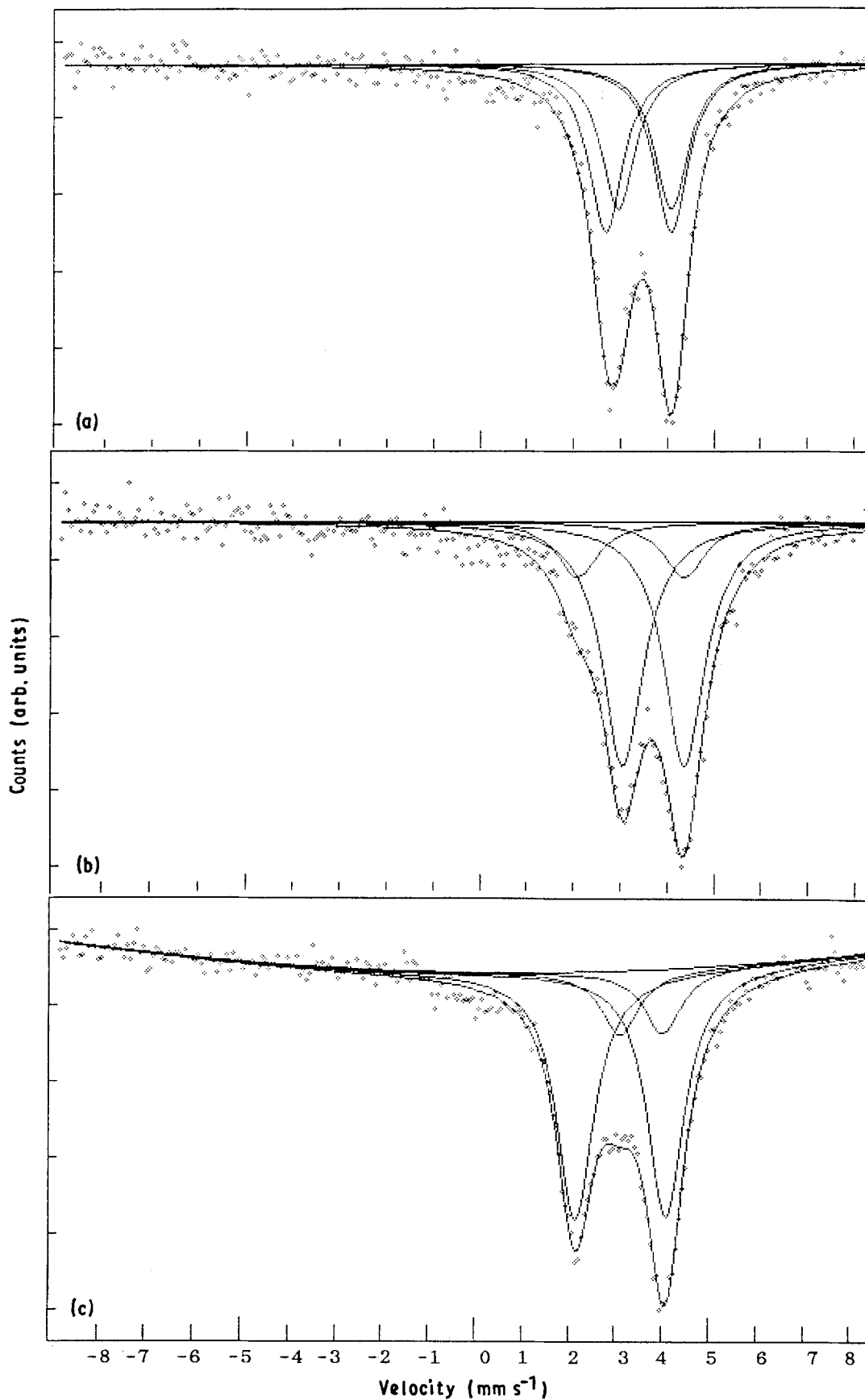


Figure 10 ^{119}Sn Mössbauer spectra of (a) tin phosphate in hureaulite, (b) tin phosphate in phosphophyllite, and (c) tin phosphate precipitated from stannous chloride solution containing tartaric acid.

properties of converted tin phosphate coatings may be estimated by analysis of the intensity ratio of Sn(II) to Sn(IV) species observed in the CEM spectra. The chemical states of tin produced in the converted tin phosphate coatings on iron and steel are complex.

Converted tin phosphate films contributed to the improvement of corrosion resistance of conventional phosphate coatings by incorporating a small-grained tin phosphate into the phosphate coating, but converted tin phosphate coatings may not always enhance

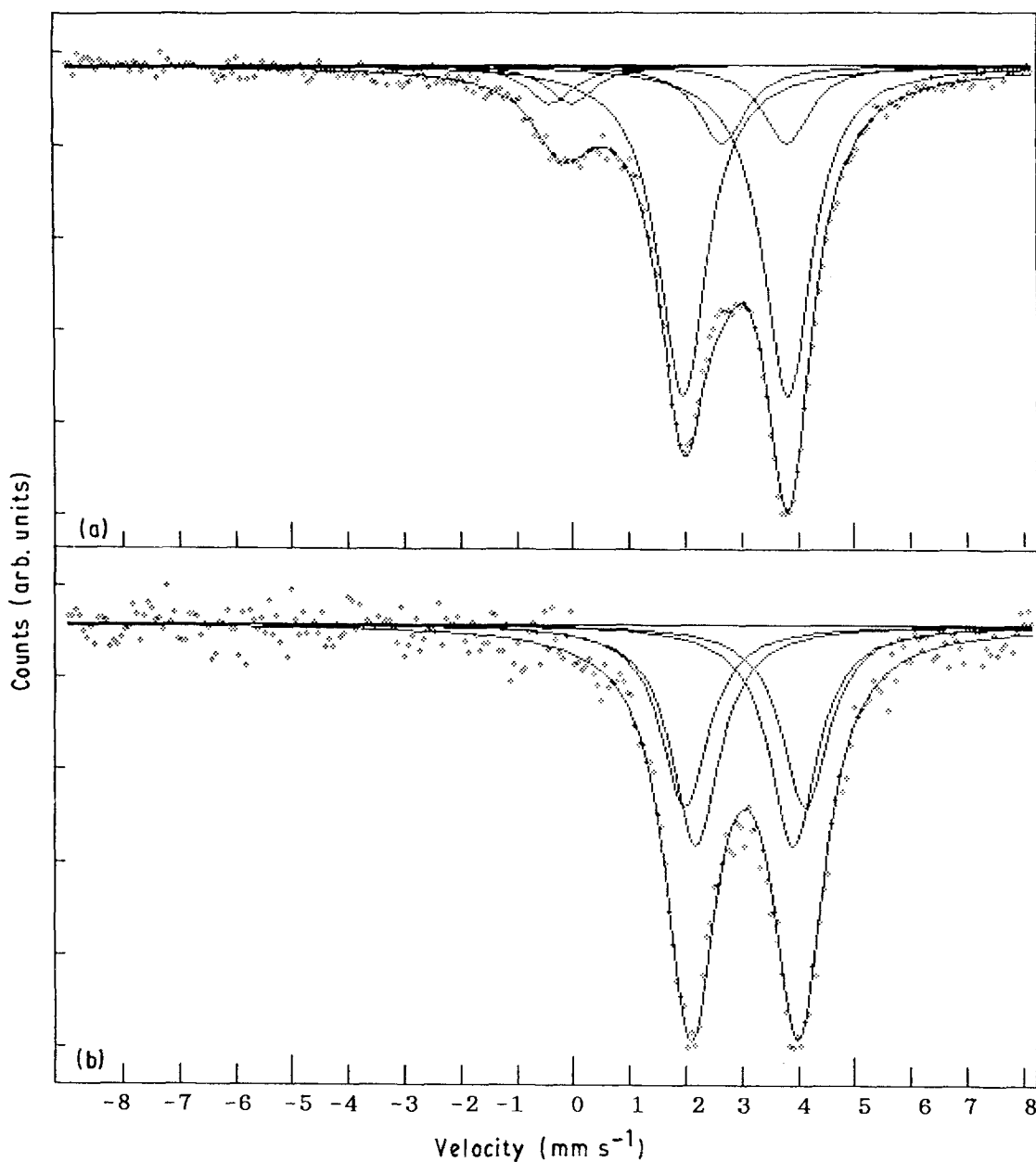


Figure 11 ^{119}Sn Mössbauer spectra of (a) tin phosphate prepared, and (b) tin phosphate heated in 5% $\text{H}_2 + \text{N}_2$ atmosphere at 810 K.

the adhesion of film to the substrate structure, from the viewpoint of the layer structure of the converted tin phosphate coatings. If tin phosphate coatings may be formed directly on iron and steel by dry processing methods such as plasma chemical vapour deposition, better quality coatings could be obtained.

References

1. G. LORIN, "Phosphating of metals" (Finishing Publications Ltd, Middlesex, 1974).
2. M. GEBHARDT, *Farb und Lack* **73** (1968) 217.
3. K. NOMURA, Y. UJIHIRA, Y. MATSUSHIMA, R. KOJIMA and Y. SUGAWARA, *Nippon Kagakukai-shi* (1980) 1372.
4. K. NOMURA and Y. UJIHIRA, *J. Anal. Appl. Pyrol.* **5** (1983) 221.
5. K. NOMURA, Y. UJIHIRA and R. KOJIMA, *Nippon Kagakukai-shi* (1982) 87.
6. K. NOMURA and Y. UJIHIRA, *ibid.* (1982) 1352.
7. *Idem*, *J. Mater. Sci.* **17** (1982) 3437.
8. E. MATTIEVICH and J. DANON, *J. Inorg. Nucl. Chem.* **39** (1977) 569.
9. B. S. TUTTLE and T. NOVOY, US Pat. 2478 954, 16 August 1949.
10. T. OYAGI, *Boseikanri* **5**(6) (1961) 17.
11. K. NOMURA and Y. UJIHIRA, *Bunsekikagaku* **33** (1984) T81.
12. R. C. MERCADER, E. J. BARAN and A. R. LOPEZ-GARCIA, *J. Radioanal. Nucl. Chem. Lett.* **85** (1984) 13.
13. J. M. FRIEDT and Y. LLABADOR, *Radiochem. Radioanal. Nucl. Chem. Lett.* **9** (1972) 237.
14. J. K. LEES and P. A. FLINN, *J. Chem. Phys.* **48** (1968) 882.

Received 15 January
and accepted 7 June 1991